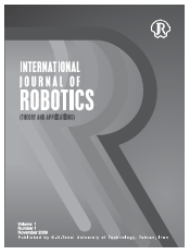

INTERNATIONAL JOURNAL OF ROBOTICS
(THEORY AND APPLICATIONS)
E-mail: IJR@kntu.ac.ir

Dynamic Modeling and Construction of a New Two-Wheeled Mobile Manipulator: Self-balancing and Climbing

S. Ebrahimi[a,*], A. Mardani[b]

[a] Associate Professor, Department of Mechanical Engineering, Yazd University, Yazd, Iran.
[b] PhD Student, Department of Mechanical Engineering, Yazd University, Yazd, Iran.

ARTICLE INFO

Article history:

Received: July 20, 2015.
Received in revised form:
September 29, 2015
Accepted: October 5, 2015.

Keywords:

Self-stability
Two-wheeled robots
Stair climbing
Mobile manipulator

ABSTRACT

Designing the self-balancing two-wheeled mobile robots and reducing undesired vibrations are of great importance. For this purpose, the majority of researches are focused on application of relatively complex control approaches without improving the robot structure. Therefore, in this paper we introduce a new two-wheeled mobile robot which, despite its relative simple structure, fulfills the required level of self-balancing without applying any certain complex controller. To reach this goal, the robot structure is designed in a way that its center of gravity is located below the wheels' axle level. The attention is more paid to obtaining a self-balancing model in which the robot's arms and other equipment follow relatively low oscillations when the robot is subjected to a sudden change. After assembling the robot using the Sim-Mechanics toolbox of Matlab, several simulations are arranged to investigate the robot ability in fulfilling the required tasks. Further verifications are carried out by performing various experiments on the real model. Based on the obtained results, an acceptable level of balancing, oscillation reduction, and power supply is observed. To promote the self-balancing two-wheeled mobile manipulator, its platform is modified to climb high obstacles. In order to obtain this aim, some transformations are done in mechanical aspects like wheels, arms and main body without any increase in DOFs. The robot is supposed to follow proposed motion calculated according to stability criteria. The kinematic equations are utilized to find a possible motion. In a dynamic simulation, the robot ability in passing over an obstacle is verified.

1. Introduction

Promotion of the robotic world is the best evidence of necessity of transforming human based missions to automatic processes based on ability of robots. Most of the peril applications are done by means of automatic devices. Mobile manipulators are used for exploring missions or industrial applications. In all applications, mathematical modeling, path planning, fluctuation elimination and using of appropriate mechanisms are necessary. Widespread researches are handled in mobile manipulator field previously [1, 2]. Stability and fluctuation elimination is the most important matters which must be investigated. In some researches, the

* Corresponding author address: Yazd University, Safayieh, Yazd, Iran.
Tel.: +983531232621; fax: +9835382112781, E-mail address: ebrahimi@yazd.ac.ir.

stability has been satisfied by mean of additional passive rollers [3, 4]. The stability investigations used in mobile manipulator field like moment height stability measure (MHS) are done [5-7]. This criterion is established on applied torques on mobile platform, the height of CG and inertia of mobile platform. Stability investigation of the dual arm suspended mobile robot has been proposed by means of MHS criterion [6]. In related researches, dynamic stability of a hybrid mobile manipulator is illustrated in [7] by means of MHS to enhance stability of platform. In other researches, force-angle measure is utilized to investigate mobile manipulator stability [8].

In these researches, application of arm and base actuators is the way to prevent over turning. Promotion of the mobile manipulators stability is done not only by means of mechanism innovation but also implementing control algorithms such as neural-fuzzy controllers [9]. In some platforms, the center of mass is moved by controller to satisfy stability criteria [10]. In recent few years, development of two-wheeled mobile manipulators has found great attention. Ha and Yuta focused on the control of a two-wheeled robot with inverse pendulum structure based on the robot velocity [11]. Grasser has provided stability for a two-wheeled mobile manipulator by means of dual state space controller [12]. In related research, a 3-DOF model of the two-wheeled robot is proposed [13]. In this paper, non-holonomic locomotion on ramps is investigated dynamically by means of dynamic approaches. In another research, the stabilization is assumed to be done by the LQR controller [14]. Some two-wheeled robot dynamic investigations are based on the Newton-Euler approach and PD controller [15]. In [16], after deriving and linearization of the dynamic equations of motion, stability control of the robot is performed using the pole placement method in real time toolbox of Matlab. A two-wheeled mobile robot with flexible links is modeled based on the combined approach of D'Alembert-Lagrange [17, 18]. Independent control of each wheel in a two-wheeled robot is proposed in [19]. In other effort, stability is investigated when the load installed on arm moves [20]. For this purpose, PD controller is utilized beside fuzzy logic. The results of simulation proof the stability under external load as disturbance force. In other control based effort [21], robust controller is utilized after extraction of dynamic equations. Motion equations are linearized about stability point of the robot arm. Then, they are rewritten into state space equations. This controller is investigated in the case of undetermined coefficient of friction. The stability control of a two-wheeled robot in tracking a prescribed path is investigated in [22]. In this case, the process of arm controlling is done by means of PD controller and optical sensors. In other paper, mobile manipulator is controlled by means of fuzzy controller based on the velocity and position [23].As a related effort, stability control of a two- wheeled mobile manipulator is analyzed on the ramps [24]. To proof the aim of this paper, the Lagrange approach is utilized. Then, Lyapunov method is used to determine stability margins. Position and velocity control process based on the optimal controller is done to satisfy stability margins. As the other effort related to the locomotion on ramp, a dynamical simulation is done in [25, 26]. Extracted equations are used to simulate locomotion on even surfaces or ramps. According to optimal control based on the optimal gains, stability of mobile manipulator is investigated. Juang and Lum [27] considered the dynamic simulation of two-wheeled robots by means of using various PID based controllers.

On an uneven surface, climbing can improve ability of locomotion. Mobile robots that can climb obstacles, or stairs have been investigated in order to generalize their missions. As a solution, the wheel of mobile manipulator can be transformed to be in [28], the body is knitted to two parts to elevate easier [29]. In other more complex solution, wheels are armed by active linkages [30]. The hybrid locomotion done by complex leg (linkage and wheel) can improve ability of climbing besides legged locomotion. Some of climbers are armed by passive linkages [31, 32]. In other efforts, 1-DOF link is deformed to the half circle shape [33, 34]. Rhex is a novel platform improved to running and climbing [35]. Some other mobile platforms are specially designed for climbing like Msrox [36, 37]. Msrox is a four-wheeled rover armed by hybrid wheels to climb stairs. The hybrid wheel composition is obtained from installing three wheels on a triangular part. Triangular part is located on each wheel connection point on the main body. In other effort, a four-wheeled robot armed by parallel mechanism is proposed to climb stair [38]. In this research, using of linkage is considered to obtain climber mechanism. As a powerful climber mechanism, a rail mobile manipulator is proposed in a hybrid structure. This mechanism is designed based on compounded duty of mobile part and manipulator part in climbing and locomotion missions [49], [40]. The research reported in [39], [40] is the first inspiration for new idea of current development to improve new mechanism proposed at the previous part of introduction. Hybrid locomotion using arm beside mobile parts is a good solution to climbing.

In this paper, we first introduce a new two-wheeled mobile robot which, despite its relative simple structure, fulfills the required level of self-balancing without applying any certain complex controller. To reach this goal, the robot structure is designed in way that its center of gravity to be located below the wheels' axle level. In the first part of this article, a newly developed self-balancing two-wheeled mobile manipulator was presented. For this purpose, the robot structure was designed in way that its center of gravity is located below the wheels' axle level. In the final model of the

robot, the attention was more paid to obtain a self-balancing model in which the robot's arms and other equipment follow relatively low oscillations when the robot is subjected to a sudden change.

In the next part of the paper, the self-balancing two-wheeled manipulator will be promoted to a climber mechanism by some changes in mechanical parts like wheels, manipulator and main body without any increasing in DOFs,. Besides mechanical transformation, stability criteria must be involved in motion planning. A proposed motion will be planned to climbing high obstacles in stability margins.

To obtain a proper platform, at the first stage, a primary virtual model of new two wheeled mobile manipulator controlled by PID controller was designed in Matlab Simulink (Sim-Mechanic) according to the primary experimental model. The aim of virtual model was detection of disadvantages of new platform specially fluctuation of locomotion. After assembling the robot using the Sim-Mechanics toolbox of Matlab, several simulations were arranged to investigate the robot ability in fulfilling the required tasks. Further verifications were carried out by performing various experiments on the real model. At the next stage, two experimental tests were considered to proof the abilities of the new platform in real locomotion. In experimental test the maximum limits of ability in obstacle crossing and ramp climbing was investigated besides fluctuation monitoring. Based on the obtained results, an acceptable level of balancing, oscillation reduction, and power supply was observed.

However, this new platform cannot continue working against high obstacles. There are many considerations must be applied on the new platform to be a successful as a mobile manipulator in performing certain missions. To eliminate the leak of ability on of climbing some virtual tests will be done to show the power of promotion of new platform to a climber robot.

2. New platform

The new platform concept is illustrated in Fig. 1.

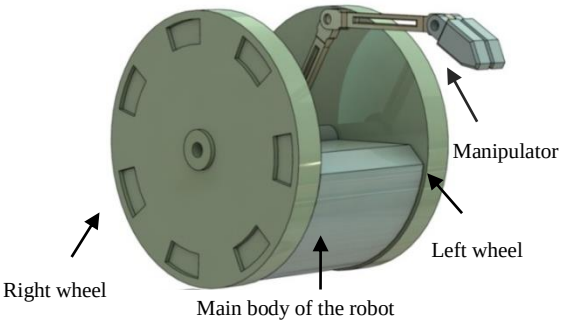

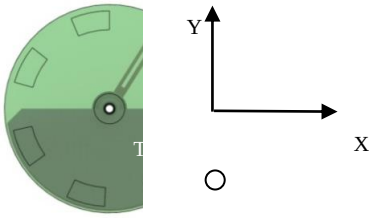

Fig. 1. Concept of platform.

As it is illustrated, mobile manipulator includes three main parts (main body, manipulator and wheels). The main body located under wheel axis allows robot to be stable permanently due to the center of gravity (CG) place which is shown in Fig. 1. A connection part including five revolute joints illustrated in Fig. 2 is designed to connect the parts of robot. As it is shown, the universal connection is a circular part that connects wheels to the manipulator arm and main body. On the other hand, connection part allows the main body and manipulator to rotate about X axis besides rotating about Y axis. This provided ability keeps robot arm coordinates vertical in ramps. A primary experimental model is fabricated to show real ability of the new mobile manipulator.

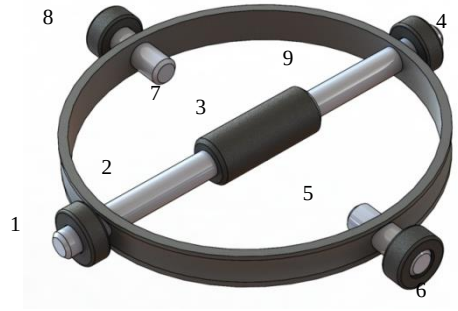

Fig. 2. Central universal joint: (1) ball bearing of the front of the robot, (2) central link to connect main body, (3) connection of main body, (4) ball bearing of the rear of robot, (5) left wheel connection, (6) ball bearing of the left wheel, (7) right wheel connection, (8) ball bearing of the right wheel, (9) connection ring of ball bearing.

As it is illustrated in Fig. 3, the first link of the manipulator is hidden under steel cover. Properties of the new model motors are provided in Table 1. There is no necessity to express properties of the control devices used in experimental model. Mechanical properties are given in Tables 4 and 5 of Appendix.

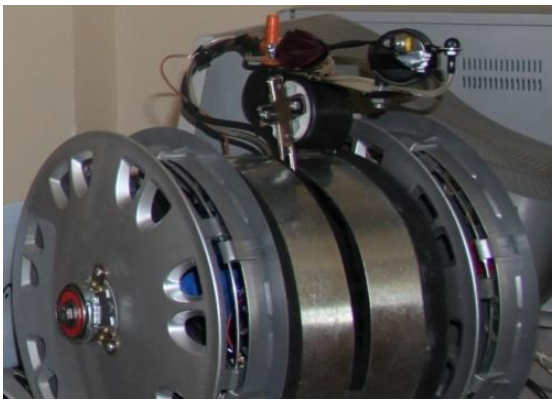

Fig. 3. Primary real model.

Table 1. The characteristic of motors

Wheel motor	Arm motor	Properties
4watt	4watt	Maximum power
9N.m	3N.m	Stall torques
60rpm	180rpm	Load less velocity
6V	6V	Voltages
0.4H	0.4 H	Inductance coefficient
0.8Ω	0.8Ω	Internal resistance
18	6	Ratio of gear box

3. Kinematics, dynamics and control

The kinematic and dynamic parameters of the 2D model are provided in Fig. 4. At the first stage, the components of CG acceleration are extracted in Eq. 1. The main assumption is non-sliding condition.

$$\begin{bmatrix} a_{1x} \\ a_{1y} \end{bmatrix} = \begin{bmatrix} r\alpha \\ 0 \end{bmatrix} + c_1 \begin{bmatrix} -\ddot{\theta}_1 \cos(\theta_1) + \dot{\theta}_1^2 \sin(\theta_1) \\ \ddot{\theta}_1 \sin(\theta_1) + \dot{\theta}_1^2 \cos(\theta_1) \end{bmatrix} \quad (1)$$

where c_1 is the center of gravity position of the main body. Determination of the first link acceleration of manipulator is expressed in Eq. 2. In the same way, Eq. 3 expresses the acceleration of the second link where $\varphi = \theta_1 + \theta_2$ and $\beta = \theta_1 + \theta_2 + \theta_3$.

$$\begin{bmatrix} a_{2x} \\ a_{2y} \end{bmatrix} = \begin{bmatrix} r\alpha \\ 0 \end{bmatrix} + c_2 \begin{bmatrix} \ddot{\varphi}\sin(\varphi) + \dot{\varphi}^2 \cos(\varphi) \\ \ddot{\varphi}\cos(\varphi) - \dot{\varphi}^2 \sin(\varphi) \end{bmatrix} \quad (2)$$

$$\begin{bmatrix} a_{3x} \\ a_{3y} \end{bmatrix} = \begin{bmatrix} r\alpha \\ 0 \end{bmatrix} + l_2 \begin{bmatrix} \ddot{\varphi}\sin(\varphi) + \dot{\varphi}^2 \cos(\varphi) \\ \ddot{\varphi}\cos(\varphi) - \dot{\varphi}^2 s\sin(\varphi) \end{bmatrix} + c_3 \begin{bmatrix} \ddot{\beta}\sin(\beta) + (\dot{\beta})^2 \cos(\beta) \\ \ddot{\beta}\cos(\beta) - (\dot{\beta})^2 \sin(\beta) \end{bmatrix} \quad (3)$$

According to Fig. 5, moment balance of the second link is driven by the Newton-Euler approach. Parameter I_3 is the mass moment of inertia of the link about CG_3. The second equation is driven by applying the recursive method in Eq. 4 according to Fig. 6.

$$\Sigma M_{O_1} = \tau_3 - m_3 g c_3 \cos(\beta) = I_3\ddot{\theta}_3 + m_3 a_{3x} c_3 \sin(\beta) + m_3 a_{3y} c_3 \cos(\beta) \quad (4)$$

$$\Sigma M_O = \tau_2 + \tau_3 - m_2 g c_2 \cos(\varphi) - m_3 g\left(l_2 \cos(\varphi) + c_3 \cos(\beta)\right) = I_2\ddot{\theta}_2 + m_2 a_{2x} c_2 \sin(\varphi) + m_2 a_{2y} c_2 \cos(\varphi) + I_3\ddot{\theta}_3 + m_3 a_{3x}\left(l_2 \sin(\varphi) + c_3 \sin(\beta)\right) + m_3 a_{3y}\left(l_2 \cos(\varphi) + c_3 \cos(\beta)\right) \quad (5)$$

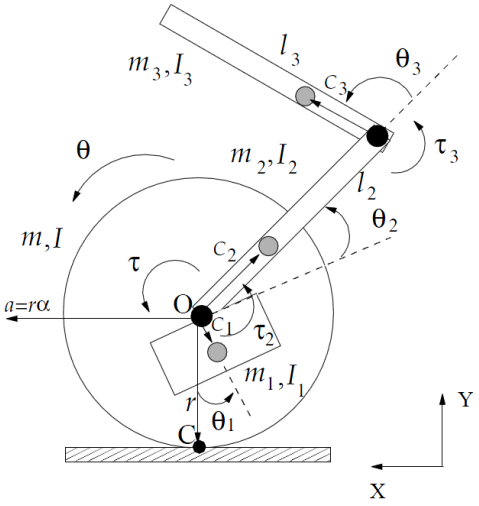

Fig. 4. Kinematic and dynamic parameters.

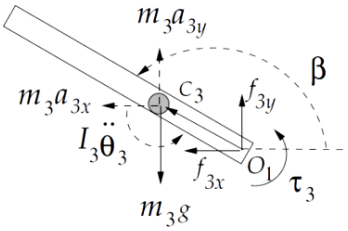

Fig. 5. The first link of manipulator.

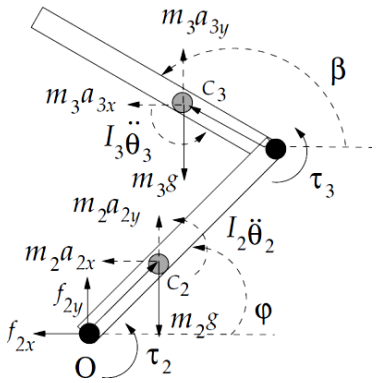

Fig. 6. Both of the first and second links.

Two other dynamic equations are driven by means of the Newton second low.

$$f_{2x} = m_2a_{2x} + m_3a_{3x}$$
$$f_{2y} - m_2g - m_3g = m_2a_{2y} + m_3a_{3y} \qquad (6)$$

The next step is extraction of the wheel equation. Eq. 7 shows the wheel equation. I_c is inertia of the wheel about point C in Fig. 4. The last step is derivation of the equations of the main body as given in Eq. 8. Figure 7 illustrates the wheel and main body properties.

$$f + f_x = ma = mr\alpha$$
$$f_y - mg + N = 0 \qquad (7)$$
$$\Sigma M_C = \tau + f_x r = I_C\alpha$$

$$-f_x - f_{2x} = m_1a_{1x}$$
$$-f_y - f_{2y} - m_1g = m_1a_{1y} \qquad (8)$$
$$\Sigma M_G = -\tau - \tau_2 + (f_y + f_{2y})c_1\sin(\theta_1) - (f_x + f_{2x})c_1\cos(\theta_1) = I_1\ddot{\theta}_1$$

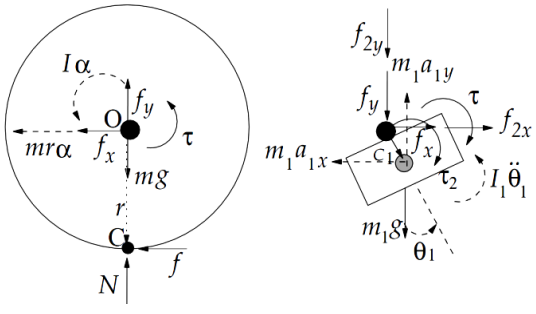

Fig. 7. Wheel and main body.

The system equations including Eqs. 4-8 consist of 10 equations which must be solved simultaneously with Eqs. 1-3. Undefined parameters are $\ddot{\theta}_2, \ddot{\theta}_3, f_x, f_y, f_{2x}, f_{2y}, f, \alpha, \ddot{\theta}_1$ and N.

Control low used in this paper is expressed in Eq. 9. According to Eq. 9, y is feedback parameter, r is control signal input, G is control signal output, N is noise elimination coefficient, and b and c are weight gains set on one. The equation is driven from [41]. The control low will be utilized for the manipulator and wheel. Fig. 8 shows the algorithm of control including Eq. 9.

$$G(s) = P(br - y) + \frac{I}{s}(r - y) + D\frac{N}{1 + \frac{N}{s}}(cr - y) \qquad (9)$$

4. Simulation and experimental efforts

This section is based on three main efforts. The first case is simulation of the robot on flat surface using Matlab Simulink (Sim-Mechanic) and its control by means of Eq. 9. The control panel of Simulink is provided in Fig. 25 of Appendix. In the second test, it is simulated in the dynamic simulation part of SolidWorks to show the ability of robot in ramp climbing. The last effort is done experimentally. In these stages, two parts are provided. The first is obstacle crossing and the second is ramp climbing. At the first stage, robot starts to move by initial condition (v = 0, a = constant and x = 0) for 8 seconds, see Fig. 9. The aim is monitoring the fluctuation of main body with respect to the fixed coordinate. Manipulator motors are supposed to be fixed. The results of angular displacement are illustrated in Fig. 10-a, for various damping coefficient of the wheel joint (B = 0.6, 1.2, 2). By choosing B = 2 according to Fig. 10-a, Fig. 10-b illustrates fluctuation of the main body with respect to the fixed coordinate system for various linear accelerations of the wheel (a = 1, 3, 5 m/s^2).

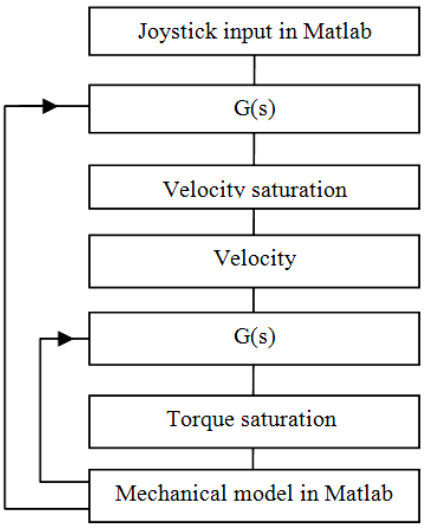

Fig. 8. Control algorithm.

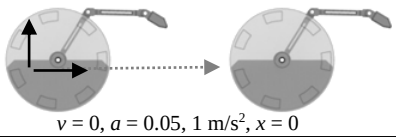

$v = 0$, $a = 0.05$, 1 m/s^2, $x = 0$

Fig. 9. Constant acceleration movement.

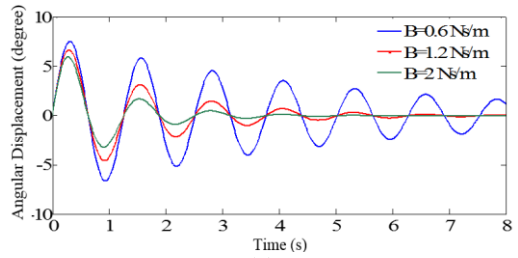

(a)

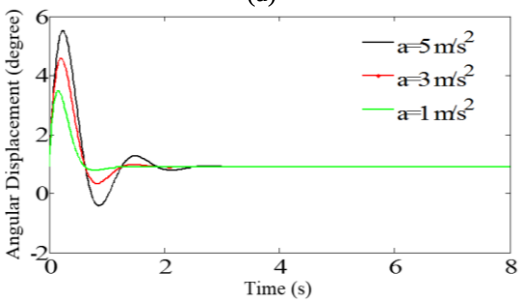

(b)

Fig. 10. Angular displacement of the main body.

Another simulation is performed in SolidWorks. In this simulation, ramp climbing will be investigated in various ramp angles ($\theta_s = 0, 15, 25, 35$ deg). Fig. 11 shows typical ramp climbing. The friction coefficient of surface is 0.4. In gentle ramps, robot climbs up properly. By increasing the value of θ_s, climbing becomes slower and in 35 degree, robot goes down in spite of climbing mission. The torque of motor is limited between 0 to 9 N.m. The results of robot displacement and also the motor torques are provided in Fig. 12.

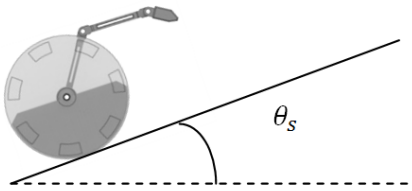

Fig. 11. Ramp climbing.

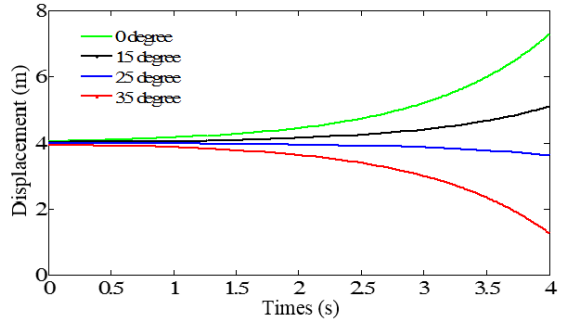

(a)

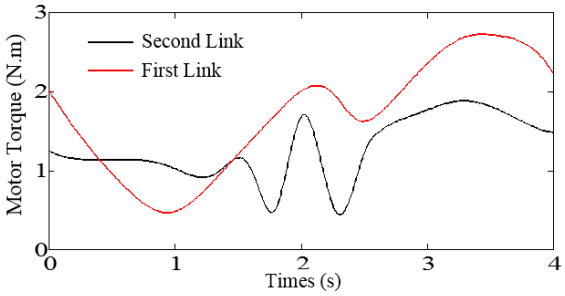

(b)

Fig. 12. Ramp climbing result

The experimental test is arranged for ramp climbing to validate the simulation results. In this test, robot is supposed to climb ramps in various slops and various friction coefficients. Table 2 expresses the result of experimental model. *S* means successful locomotion and *N* is failed test.

In other experimental test, the robot is supposed to cross obstacles (Fig. 13). The test is managed in various heights of obstacle (0.05, 0.1, 0.12, 0.16 *m*). Furthermore, in another effort, new flexible belt with pretension is used in manipulator links to reduce the effect of gravity and fluctuations on the arm motors as illustrated in Fig. 14.

Table 2. Slop climbing result

Slop=10	Slop=15	Slop=20	Slop=25	Friction coefficient
S	S	N	N	0.1
S	S	S	N	0.2
S	S	S	S	0.4

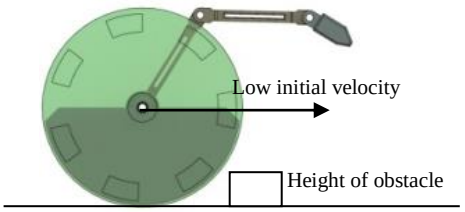

Fig. 13. Obstacle crossing.

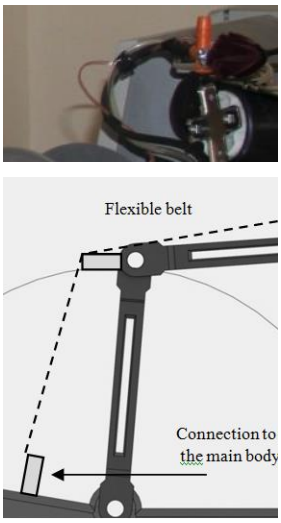

Fig. 14. Flexible belt with pretension.

According to the results of Table 3, robot cannot pass the 0.16*m* obstacle without flexible belt, which in the case of using the flexible belt, it can pass the obstacle.

Table 3. Obstacle climbing

Obstacle height	0.05	0.1	0.12	0.16
Crossing without flexible belt	S	S	S	N
Crossing with flexible belt	S	S	S	S

5. Promotion to the climber model

The newly developed platform can further be modified to be a climber mobile manipulator. The main body shape and manipulator are modified as shown in Fig. 15. The wheels are reconstructed by adding jagged surface. Fig.15 (a-1) is the primary new platform and (a-2) is the modified platform armed by jagged wheels. Fig. 15 (b-1) shows the primary form of the main body where (b-2) shows modified shape of the main body. Figs. 15 (c-1) and (c-2) present the primary and the modified manipulators, respectively. The ability of climbing will be investigated.

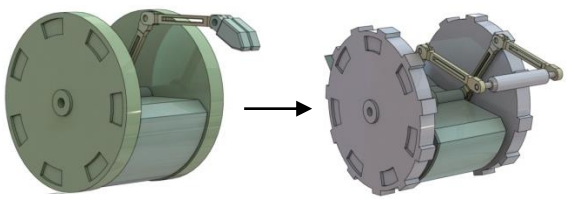

(a-1) (a-2)

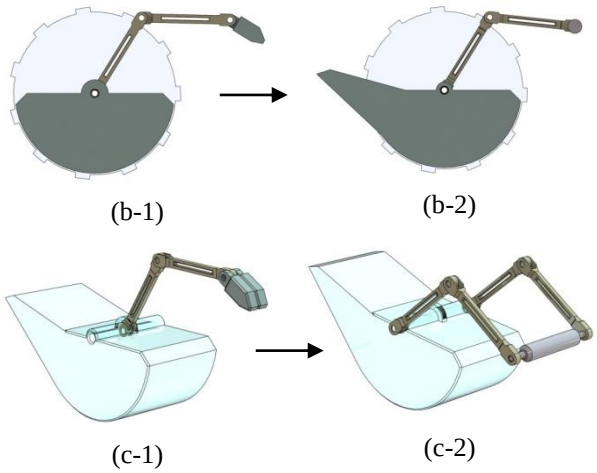

(b-1) (b-2)

(c-1) (c-2)

Fig. 15. Modified platform.

The main contact points by ground are illustrated in Fig. 16 as C_1 the contact point of tail, C_2 the contact point of wheel and C_3 the contact point of the manipulator end-point. The aim of improvement of manipulator structure is to obtain collision ability against ground. The tail is added to platform to provide collision ability against environment. Indeed, in motion planning, tail and end-point are the essential points for climbing.

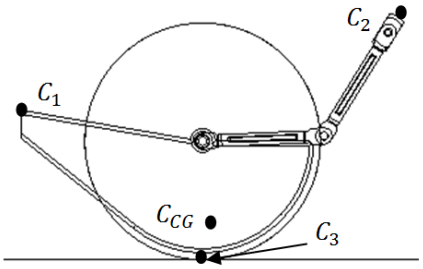

Fig. 16. Main points of climbing.

The main idea is that when the end-point of the manipulator is locked by ground collision and friction force, the main body starts to rotate instead of manipulator. In this way, by engaging both the end-point and tail of the robot in climbing, the robot can perform the required task.

6. Stability margins

The essential constraint of climbing is to be stable permanently. Many types of stability criterion have been proposed. In this paper, the criterion is horizontal distance between center of gravity (CG) point and ground contact points. In fact, CG point must be located between two contact points during motion, as shown in

Fig. 17. This criterion demonstrates stability and overturning prevention. A special stability point is when the robot CG is located under wheel axis. Mobile manipulator is permanently stable due to the results of self-balancing part. A typical position is shown in Fig. 17 to illustrate stability margins. In this figure, D_{C1} and D_{C2} are stability margins. If they became less than zero, the platform starts to overturn. So, all the motion planning tasks must adopt positive amount of stability margins.

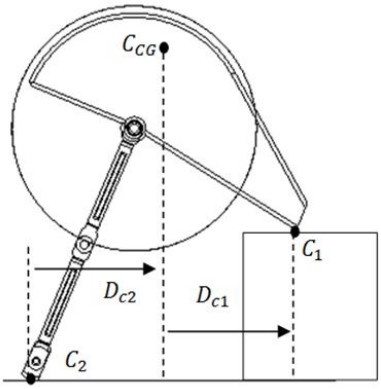

Fig. 17. Stability margins.

7. Motion planning

The goal of platform modification presented is that the robot can pass over the obstacles with height more than wheel radius. In the case of obstacles with height less than the wheel radius, no further modification addition to the already developed robot platform is needed. After modification, a motion planning must be done in stability margins mentioned previously. The required steps of the obstacle climbing are illustrated in Fig. 18. In steps 1 and 2, the first link rotates until it collides the ground. In step 3, the second link contact with ground remains due to ground friction. In this step, the main body rotates as illustrated in Fig. 18. This step is continued until the tail collides the obstacle as shown in Fig. 18. In step 5, the collision between wheel and obstacle occurs by rotating the second link. Now, the robot is ready to rotate its wheel to climb finally. In step 6, the wheel rotates and the robot climbs obstacle. In step 6, the tail starts sliding on the top of obstacle and center of wheel starts to move toward horizontal axis. In this stage, the end-effector of the manipulator leaves the ground.

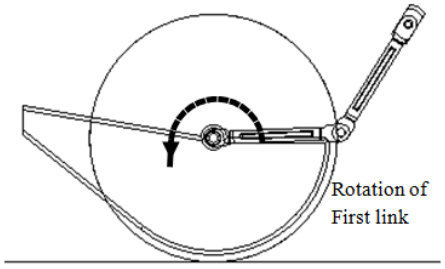

Step 1

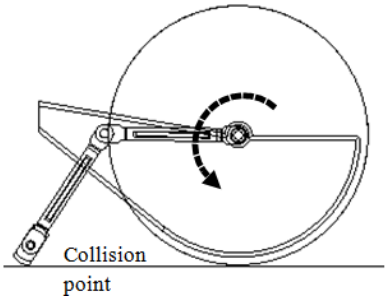

Step 2

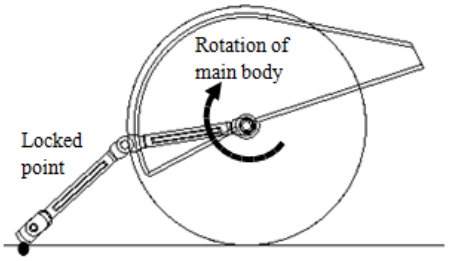

Step 3

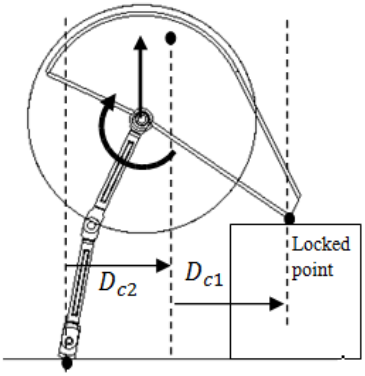

Step 4

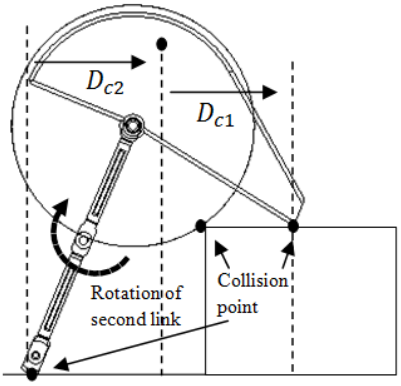

Step 5

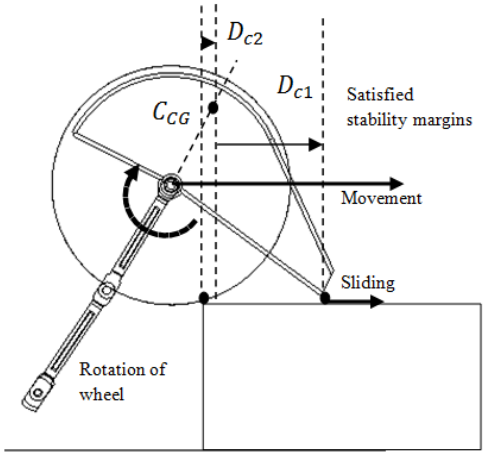

Step 6

Fig. 18. Required steps of obstacle climbing.

8. Kinematic and stability equations

The kinematic parameters are identified in Fig. 19. In this figure, θ_b, θ_1 and θ_2 are angles of the main body with respect to the fixed coordinate, angle of the first link with respect to the main body, and angle of the second link with respect to the first link, respectively.

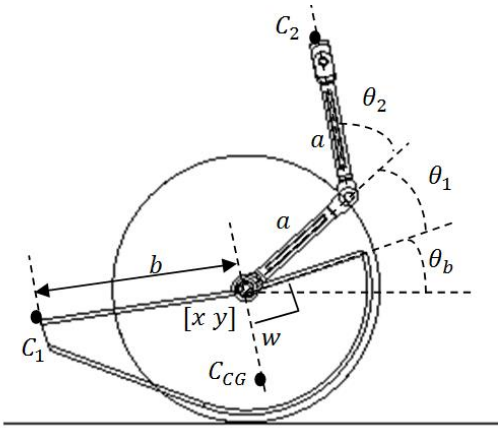

Fig. 19. Kinematic parameters.

Variables x and y express the position coordinates of the wheel's gravity center, and w is the distance between wheel center and *CG*. Eqs. 10-12 describe the position of contact points C_1 and C_2, and robot center of gravity C_{CG}.

$$C_1 = \begin{bmatrix} x + b\cos(\pi + \theta_b) \\ y + b\sin(\pi + \theta_b) \end{bmatrix} \tag{10}$$

$$C_2 = \begin{bmatrix} x + a(\cos(\theta_b + \theta_1) + \cos(\theta_b + \theta_1 + \theta_2)) \\ y + a(\sin(\theta_b + \theta_1) + \sin(\theta_b + \theta_1 + \theta_2)) \end{bmatrix} \tag{11}$$

$$C_{CG} = \begin{bmatrix} x + w\cos(3\pi/2 + \theta_b) \\ y + w\sin(3\pi/2 + \theta_b) \end{bmatrix} \tag{12}$$

The stability margins D_{C1} and D_{C2} introduced in Fig. 18 can now be expressed by Eq. 13. The motion planning criteria must satisfy Eq. 13 which explains the stability condition.

$$\begin{aligned} &\text{if } C_{1y} < C_{2y} \rightarrow \begin{cases} D_{C1} = C_{CG\_y} - C_{1y} \\ D_{C2} = -C_{CG\_y} + C_{2y} \end{cases} \\ &\text{if } C_{2y} < C_{1y} \rightarrow \begin{cases} D_{C1} = -C_{CG\_y} + C_{1y} \\ D_{C2} = C_{CG\_y} - C_{2y} \end{cases} \end{aligned} \tag{13}$$

A proposed motion satisfying stability margins is numerically identified and illustrated in Fig. 20. Variations of the corresponding stability margins required for a stable obstacle climbing are shown in Fig. 21. The important matter is that the value of D_{C1} is negative until t = 2s as illustrated with a vertical line. The required stability condition is that all stability margins must be positive. Until this time, CG height is lower than the wheel axis. It was mentioned previously that the stability margins are not required in this condition and the robot is self-stable. In this condition, the wheel has contact by ground. When tail point C_1 is out of the stability margin, the wheel contact point keeps the platform in stable condition (between t=0 and t = 3.7 s). This matter is obvious in Fig. 18, steps 2, 3 and 4. After t=3.7 s, the wheel leaves the ground and tail collides the obstacle. After this time, the tail roles to keep stable condition according to the stability conditions of Eq. 13.

9. Dynamic simulation

Simulation of the climbing obstacle in the modified robot platform is carried out. Fig. 22 shows the climbing steps. At the end of Fig. 22, the path created by the robot wheel center is shown. The modified mobile manipulator can overcome the obstacle according to

Fig. 22. The motion utilized in simulation is the motion planned in Figs. 20 and 21.

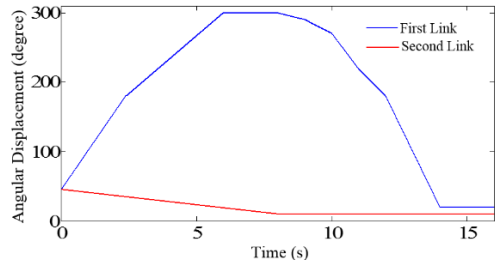

(a)

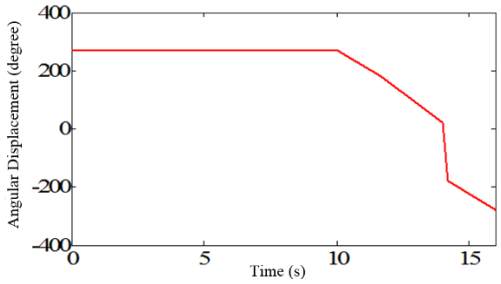

(b)

Fig. 20. Proposed steps of climbing angels,(a): angles of the manipulator links, (b): wheel angle.

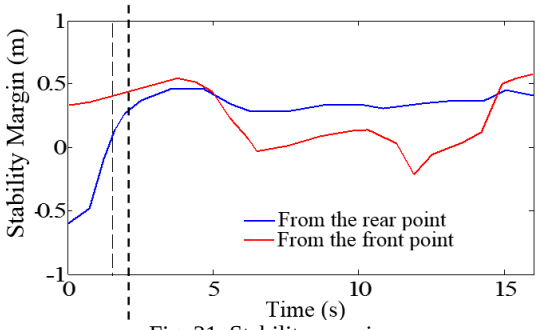

Fig. 21. Stability margins.

Dynamic simulation is done in dynamic simulation part of the SolidWorks. Dynamic and geometric properties are provided in Tables 4 and 5 of Appendix. The results of dynamic simulation proof the ability of climbing. Figure 23 shows displacement of the wheel center, which clearly states that the mobile robot finally climbs the obstacle and elevates about 30 cm.

Furthermore, Fig. 24 shows variation of the motor torques. According to this figure, the range of absolute torques is between -40 and 70 *N.m*. The first link uses the most torque between all motors. Indeed, powerful motors are required in this modified platform.

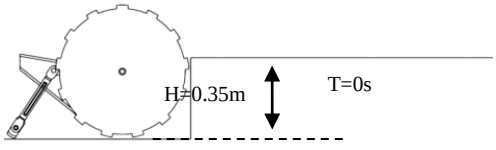

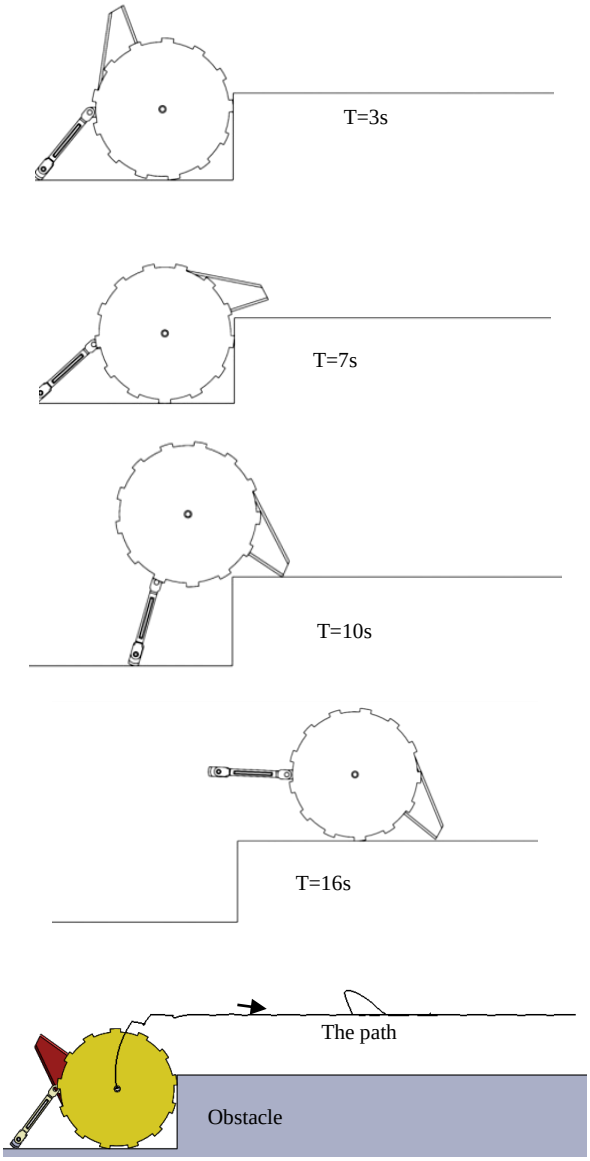

Fig.22. Obstacle climbing.

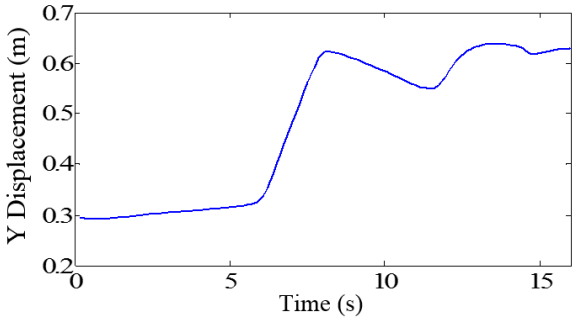

Fig. 23. Y displacement of the center of manipulator.

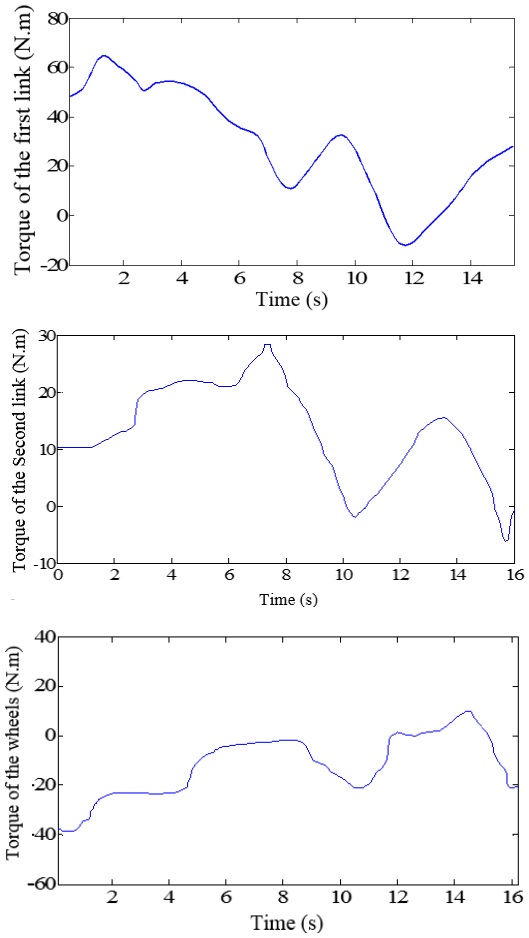

Fig. 24. Torque of motors.

10. Conclusion

The steps of mechanical designing, primary experimental model fabrication, and derivation of the dynamic equations and simulations of the virtual and real models were the main efforts done in this paper. To obtain a proper platform, at the first step, a primary virtual model of the new two-wheeled mobile manipulator controlled by PID controller was designed in Matlab Simulink (Sim-Mechanic) according to the primary experimental model. The aim of virtual model was detection of disadvantages of the new platform specially fluctuation of locomotion. At the last step, two experimental tests were carried out to proof the abilities of the new platform in real model. In experimental test, the maximum limits of ability in obstacle crossing and ramp climbing was investigated besides fluctuation monitoring. Then, the newly developed self-balancing two-wheeled mobile manipulator of Part I of this article was modified to climb high obstacles. The new idea is inspired from the study results of [12] and also Part I of this paper. According to the results, a motion was planned satisfying stability margins during climbing mission. The motion was applied on a virtual dynamic model. According to the obtained results, the virtual model followed the prescribed motion and reached top of the obstacle. The results proof the ability of the newly modified robot in climbing. An important matter is that the new platform needs powerful motors to handle missions of climbing.

References

[1] S. Zhou, Y. C. Pradeep and P. C. Chen, "Simultaneous base and end-effector motion control of a nonholonomic mobile manipulator", *In Automation, Robotics and Applications* (*ICARA*), (2015), pp. 143–148.

[2] R. Siegwart and I. R. Nourbakhsh, "Introduction to Autonomous Mobile Robots", Second Edition, The MIT Press. (2011).

[3] R. L. Williams, B. E. Carter, P. Gallina and G. Rosati. "Dynamic Model with Slip for Wheeled Omni-directional Robots", *IEEE Transactions on Robotics and Automation*, Vol. 18, (2002), pp. 285–293.

[4] K. Watanabe, Y. Shiraishi, S. G. Tzafestas, J. Tang and T. Fukuda, "Feedback. Control of an Omnidirectional Autonomous Platform for Mobile Service Robots", *Journal of Intelligent Robotic Systems*, Vol. 22, (1998), pp. 315–30.

[5] S. A. A. Moosavian and K. Alipour, "On the Dynamic Tip-Over Stability of Wheeled Mobile Manipulators", *International Journal of Robotics and Automation*, Vol. 22, (2007), pp. 322–328.

[6] S. A. A. Moosavian, K. Alipour and Y. Bahramzadeh, "Dynamics Modeling and Tip-Over Stability of Suspended Wheeled Mobile Robots with Multiple Arms", Proceedings of the IEEE/RSJ International Conference on Intelligent Robots and Systems, San Diego, USA, (2007), pp. 1210–1215.

[7] S. A. A. Moosavian and S. S. Hoseyni, "Dynamic Modeling and Tipover Stability of a Hybrid Serial-Parallel Mobile Robot", The 2nd International Conference on Control, Instrumentation, and Automation (ICCIA), Shiraz, Iran, (2011).

[8] C. L. Cham and W. H. Tan, "Design of an intelligent electronic system for dump truck tip-over prevention", *Informacije midel-journal of microelectronics electronics components and materials*, Vol. 44, (2014), pp. 152-158.

[9] A. Ghaffari, A. Meghdari, D. Naderi and S. Eslami, "Tip-over Stability Enhancement of Wheeled Mobile Manipulators Using an Adaptive Neuro-Fuzzy Inference Controller System", *International Journal of Information and Mathematical Sciences*, Vol. 5, (2009), pp. 211–217.

[10] R. C. Ooi, "Balancing a Two-Wheeled Autonomous Robot. Master Thesis, School of Mechanical Engineering", The University of Western Australia, Crawley, (2003).

[11] Y. Ha and S. Yuta, "Trajectory tracking control for navigation of the inverse pendulum type self-contained mobile robot", *Robotics and Autonomous Systems*, Vol. 17, (1996), pp. 65–80.
[12] F. Grasser, A. D'Arrigo, S. Colombi and A. C. Rufer, "JOE: a mobile, inverted pendulum", *IEEE Transactions in Industrial Electronics*, Vol. 49, (2002), pp. 107–114.
[13] Y. Kim, S. H. Kim and Y. K. Kwak, "Dynamic Analysis of a Nonholonomic Two-Wheeled Inverted Pendulum Robot", *Journal of Intelligent and Robotic Systems*, Vol. 44, (2005), pp. 25–46.
[14] W. An and Y. Li, "Simulation and Control of a Two-wheeled Self-balancing Robot", Proceeding of the IEEE International Conference on Robotics and Biomimetics (ROBIO), Shenzhen, China, (2013).

[15] K. M. Goher and M. O. Tokhi, "Modeling Simulation and Balance Control of a Two-Wheeled Robotic Machine with Static Variation in Load Position", In the Proceedings of the 22nd European Conference on Modeling and Simulation, Nicosia, Cyprus, (2008).

[16] S. W. Nawawi, M. N. Ahmad and J. H. S. Osman, "Real-Time Control of a Two-Wheeled Inverted Pendulum Mobile Robot", *World Academy of Science, Engineering and Technology*, Vol. 15, (2008), pp. 214–220.
[17] X. Raun, H. Ren, X. Li and Q. Wang, "Dynamic Model and Analysis of the Flexible Two-Wheeled Mobile Robot", *Intelligent Robotics and Applications*, Vol. 5314, (2008), pp. 933– 942.
[18] X. Raun and J. Zhao, "The Flexible Two-Wheeled Self-balancing Robot based on Hopfield", *Intelligent Robotics and Applications*, Vol. 5928, (2009), pp. 1196– 1204.
[19] P. Genova, M. Mihailova, R. Oransky and D. Ignatova, "Kinematics And Dynamics Modelling of Two-Wheeled Robot", 11th National Congress on Theoretical and Applied Mechanics, 2-5 Sept., Borovets, Bulgaria, (2009).

[20] K. M. Goher, M. O. Tokhi and N. H. Siddique, "Dynamic Modeling and Control of A Two Wheeled Robotic Vehicle With A Virtual Payload", *ARPN Journal of Engineering and Applied Sciences*, Vol. 6, (2011), pp. 7–41.

[21] L. Mollov and P. Petkov, "Embedded Robust Control of Self-balancing Two-wheeled Robot", *Information Technologies and Control*, Vol. 4, (2011), pp. 23–31.

[22] N. M. Abdul Ghani, F. Naim and T. P. Yon, "Two Wheels Balancing Robot with Line Following Capability", *World Academy of Science, Engineering and Technology*, Vol. 55, (2011), pp. 634-638.

[23] J. Wu, W. Zhang and S. Wang, "A Two-Wheeled Self-Balancing Robot with the Fuzzy PD Control Method", *Mathematical Problems in Engineering*, Vol. 2012, Article ID 469491, (2012).

[24] K. Peng, X. Ruan and G. Zuo, "Dynamic model and balancing control for two-wheeled self-balancing mobile robot on the slopes", 10th World Congress on Intelligent Control and Automation (WCICA), Beijing, (2012), pp. 3681 – 3685.

[25] Z. Kausar, K. Stol and N. Patel, "The Effect of Terrain Inclination on Performance and he Stability Region of Two-Wheeled Mobile Robots", *International Journal of Advanced Robotic Systems*, Vol. 9, (2012), pp. 1–11.
[26] T. Tomašić, A. Demetlika ans M. Crneković, "Self-Balancing Mobile Robot Tilter", *Transactions of Famena*, Vol.3, (2012), pp. 23–32.
[27] H. S. Juang, K. Y. Lum, "Design and Control of a Two-Wheel Self-Balancing Robot using the Arduino Microcontroller Board", 10th IEEE International Conference on Control and Automation (ICCA), Hangzhou, China, (2013).
[28] J. M. Morrey, B. Lambrecht, , A. D. Horchler, R. E. Ritzmann and R. D. Quinn, "Highly mobile and robust small quadruped robots", *Intelligent Robots and Systems*, Vol. 1, (2003), pp. 82-87.
[29] A. S. Boxerbaum, P. Werk, R. D. Quinn and R. Vaidyanathan, "Design of an autonomous amphibious robot for surf zone operation: part I mechanical design for multi-mode mobility", *Advanced Intelligent Mechatronics. Proceedings*, 2005 IEEE/ASME International Conference, (2005), pp. 1459-1464.
[30] A. Halme, I. Leppänen , S. Salmi and S. Ylönen, "Hybrid locomotion of a wheel-legged machine", 3rd Int. Conference on Climbing and Walking Robots, (2000).
[31] R. Volpe, J. Balaram, T. Ohm and T. Ivlev, "The Rocky 7 Mars Rover Prototype", IEEE/RSJ International Conference on Intelligent Robots and Systems, Osaka Japan, (1996).
[32] T. Estier, Y. Crausaz, B. Merminod, M. Lauria and R. R. Siegwart, "An innovative Space Rover with Extended Climbing Alilities". Proceedings of Space and Robotics, (2000).
[33] H. Tappeiner, S. Skaff, , T. Szabo and R. Hollis, "Remote haptic feedback from a dynamic running machine. Robotics and Automation", IEEE International Conference, (2009), 2368-2373.
[34] N. Neville, M. Buehler and I. Sharf, "A bipedal running robot with one actuator per leg. Robotics and Automation", ICRA (2006), pp. 848-853.
[35] S. C. Chen, K. J. Huang, W. H. Chen, S. Y. Shen, C. H. Li and P. C Lin, "Quattroped: A Leg-Wheel Transformable Robot", *Mechatronics, IEEE/ASME Transactions* Vol. 2, (2014), pp. 730-742.
[36] M. M. Dalvand and M. M. Moghadam, "Stair climber smart mobile robot (MSRox)", *Autonomous Robots*, Vol. 20, (2002), pp. 3-14.

[37]M. M. Dalvand and M. M. Moghadam, "Design and modeling of a stair climber smart mobile robot (MSRox)", ICAR Proceedings of the 11th International Conference on Advanced Robotics, (2003), pp. 1062-1067.
[38] O. Matsumoto, S. Kajita, K. Tani, and M. Oooto, "A four-wheeled robot to pass over steps by changing running control modes", *Robotics and Automation*, Vol. 2, (1995), pp. 1700-1706.
[39] P. Ben-Tzvi, A. A. Goldenberg, and J. W Zu, "Design and analysis of a hybrid mobile robot mechanism with compounded locomotion and manipulation capability", *Journal of Mechanical Design*, Vol. 7, (2008).
[40] P. Ben-Tzvi, S. Ito and A. Goldenberg, "Autonomous stair climbing with reconfigurable tracked mobile robot", *Robotic and Sensors Environments. International Workshop*, (2007), pp. 1-6.
[41] Matlab Simulink, PID control Toolbox.

Biography

Saeed Ebrahimi is currently an associate professor of Mechanical Engineering at Yazd University, Iran. He has received his PhD in Mechanical Engineering from Stuttgart University, Germany, in 2007. He has also completed his postdoctoral fellowship at the Center for Intelligent Machines (CIM), McGill University in 2008. His current research interest includes Dynamic Modelling of Multibody Systems, Robotics, Mechanisms Design and Vibration Analysis of Mechanical Systems.

Arman Mardani is currently a PhD student in the Department of Mechanical Engineering at Yazd University. He received his BSc in Mechanical Engineering in 2012 from Yazd University and his MSc in Mechatronic Engineering in 2014 from Shahrood University. His research interests include robotics, structural design of robots and multibody simulations related to multimode and mobile robots.

Appendix

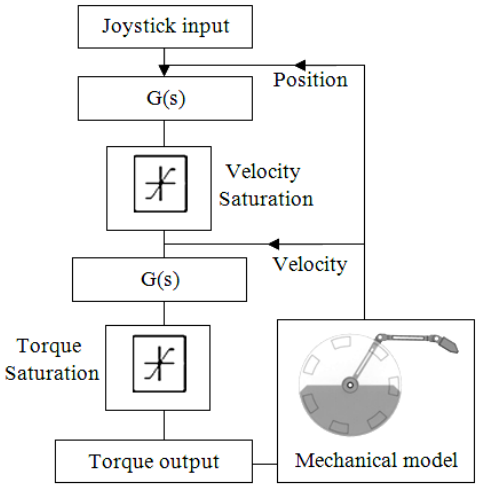

Fig. 25. Matlab Simulink diagram.

Table 4. Mechanical properties

Part	Property	Value
Manipulator link	length	0.2 m
Manipulator link	mass	0.3 kg
Main body	mass	20 kg
Wheel	radius	0.275 m
Wheel	mass	0.2 kg
Wheel	width	0.03 m
Axis	length	0.3 m

Table 5. Self-stable robot properties

Property	Value
a	0.2 m
b	0.4 m
w	0.255 m
r	0.275 m
Link mass	0.3 kg
Wheel mass	1 kg
Main body mass	20 kg
Friction coefficient	0.45